ditions at frequencies less than 100 MHz [4]. This is because muscle is primarily resistive below 100 MHz; the loss tangent (the ratio of the loss factor to the dielectric constant) increases from 2.1 at 100 MHz to 5.8 at 13.56 MHz for dog skeletal muscle [5]. Others have used phantoms simulating both the dielectric constant and the conductivity of muscle at frequencies below 100 MHz [7]–[9], and the new mixtures described may also be considered in applications requiring complete simulation of the dielectric properties of muscle.

We do not report thermal properties of these new tissue-simulating materials. However, other phantom materials [30] and diverse biological materials [31] with high water content have heat capacities and thermal conductivity values close to those of pure water, and we expect that the materials described here will as well. For precise studies involving calorimetry, the heat capacity of any phantom should be measured directly by the investigator.

References

[1] A. W. Guy, M. D. Webb, and C. C. Sorenson, "Determination of power absorption in man exposed to high frequency electromagnetic fields by thermographic measurements on scale models," *IEEE Trans. Biomed. Eng.*, vol. BME-23, pp. 361–371, Sept. 1976.

[2] M. A. Stuchly, S. S. Stuchly, and G. Kantor, "Diathermy applicators with circular aperture and corrugated flange," *IEEE Trans. Microwave Theory Tech.*, vol. MTT-28, pp. 267–271, Mar. 1980.

[3] J. R. Oleson, "Hyperthermia by magnetic induction: I. physical characteristics of the technique," *Int. J. Radiation Oncology/Biology/Physics*, vol. 8, pp. 1747–1756, Oct. 1982.

[4] A. G. Visser, G. C. Van Rhoon, P. M. Van Den Berg, and H. S. Reinhold, "Evalulation of calculated temperature distributions for a 27 MHz ridged waveguide used in localized deep hyperthermia," *Int. J. Hyperthermia*, vol. 3, pp. 245–256, May–June 1987.

[5] R. D. Stoy, K. R. Foster, and H. P. Schwan, "Dielectric properties of mammalian tissues from 0.1 to 100 MHz: A summary of recent data," *Physics in Medicine & Biology*, vol. 27, pp. 501–513, Apr. 1982.

[6] K. R. Foster and H. P. Schwan, "Dielectric properties of tissues—A critical review," *CRC Critical Reviews in Bioengineering*, vol. 17, pp. 25–104, 1989.

[7] M. A. Stuchly and S. S. Stuchly, "Dielectric properties of biological substances—Tabulated," *J. Microwave Power*, vol. 15, no. 1, pp. 19–26, 1980.

[8] C. K. Chou, G-W-Chen, A. W. Guy, and K. H. Luk, "Formulas for preparing phantom muscle tissues at various radio frequencies," *Bioelectromagnetics*, vol. 5, no. 4, pp. 435–441, 1984.

[9] T. W. Athey, J. B. Leonard and D. Giroux, "Improved phantom materials for use at shortwave frequencies," in *Bioelectromagnetic Society Sixth Annual Meeting Program and Abstracts*, Atlanta, GA, 1984, p. 23, July 15–19.

[10] G. W. Hartsgrove, A. Kraszewski and A. Surowiec, "Simulated biological materials for electromagnetic radiation absorption studies," *Bioelectromagnetics*, vol. 8, no. 1, pp. 29–36, 1987.

[11] W. J. Kopecky, "Using liquid dielectrics to obtain spatial thermal distributions," *Medical Physics*, vol. 7, pp. 566–570, Sept./Oct. 1980.

[12] J. L. Guerquin-Kern, M. J. Hagmann, and R. L. Levin, "Experimental characterization of helical coils as hyperthermia applicators," *IEEE Trans. Biomed. Eng.*, vol. 35, pp. 46–52, Jan. 1988.

[13] M. J. Hagmann and R. L. Levin, "Coupling efficiency of helical coil hyperthermia applicators," *IEEE Trans. Biomed. Eng.*, vol. BME-32, pp. 539–540, July 1985.

[14] R. Furth, "Dielektrizitatskonstanten einiger Wabriger Losungen und ihre Deutung nach der Dipoltheorie von Debye," *Annalen Der Physik*, vol. 70, no. 1, pp. 63–80, 1923.

[15] E. A. Harrington, "The dielectric constant of aqueous solutions," *Phys. Rev.*, vol. 8, pp. 581–594, Dec. 1916.

[16] P. S. Albright, "Experimental tests of recent theories descriptive of the salting out effect," *J. Amer. Chem. Soc.*, vol. 59, pp. 2098–2104, Nov. 1937.

[17] G. R. Leader, "The dielectric constant of formamide," *J. Amer. Chem. Soc.*, vol. 73, pp. 856–857, Feb. 1951.

[18] E. H. Grant, R. J. Sheppard, and G. P. South, *Dielectric Behavior of Biological Molecules in Solution.* Oxford, Clarendon Press, 1978, p. 173.

[19] G. R. Leader and J. F. Gormley, "The dielectric constant of N-methylamides," *J. Amer. Chem. Soc.*, vol. 73, pp. 5731–5733, Dec. 1951.

[20] R. A. Hovermale, P. G. Sears, and W. K. Plucknett, "Polarizations and refractions of some N-methylacetamide-n-alcohol systems," *J. Chem. Eng. Data*, vol. 8, pp. 490–493, Oct. 1963.

[21] C. H. Durney, C. C. Johnson, and H. Massoudi, "Long-wavelength analysis of planewave irradiation of a prolate spheroid model of man," *IEEE Trans. Microwave Theory Tech.*, MTT-23, pp. 246–253, Feb. 1975.

[22] A. Feldman, M. Hagmann, T. Roelofs, P. Weaver, C. Ibana, and A. Maturan, "Heating pattern of a single-loop applicator buried in muscle-equivalent phantom material measured at S-band," *Cancer Letters*, vol. 23, pp. 73–79, May 1984.

[23] J. L. Guerquin-Kern, "Hyperthermie locale par micro-ondes en therapeutique cancerologique," Doctoral thesis, Universite Louis Pasteur de Strasbourg, Strasbourg, France, June 1980.

[24] M. G. Bini, A. Ignesti, L. Millanta, R. Olmi, N. Rubino and R. Vanni, "The polyacrylamide as a phantom material for electromagnetic hyperthermia studies," *IEEE Trans. Biomed. Eng.*, vol. BME-31, pp. 317–322, Mar. 1984.

[25] S. S. Stuchly, M. A. Rzpecka, and M. F. Iskander, "Permittivity measurements at Microwave Frequencies using Lumped Elements," *IEEE Trans. Instrum. Meas.*, vol. IM-23, pp. 56–62, Mar. 1974.

[26] M. W. Aaron and E. H. Grant, "Dielectric relaxation of glycine in water," *Trans. Faraday Soc.*, vol. 59, no. 1, pp. 85–89, 1963.

[27] J. W. Hand, J. E. Robinson, S. Szwarnowski, R. J. Sheppard, and E. H. Grant, "A physiologically compatible tissue-equivalent liquid bolus for microwave heating of tissues," *Physics in Medicine & Biology*, vol. 24, pp. 426–431, Mar. 1979.

[28] K. R. Foster, E. Cheever, J. B. Leonard, and F. D. Blum, "Transport properties of polymer solutions: A comparative approach," *Biophys. J.*, vol. 45, pp. 975–984, May 1984.

[29] *CRC Handbook of Chemistry and Physics*, 63rd ed., CRC Press, Boca Raton, FL, 1982–1983.

[30] J. B. Leonard, K. R. Foster, and T. W. Athey, "Thermal properties of tissue equivalent phantom materials," *IEEE Trans. Biomed. Eng.*, vol. BME-31, pp. 533–536, July 1984.

[31] H. J. Bowman, E. G. Cravalho, and M. Woods, "Theory, Measurements and Application of Thermal Properties of Biomaterials," *Annual Review of Biophysics and Bioengineering*, vol. 4, pp. 43–80, 1975.

Microstrip Resonators on Anisotropic Substrates

Thinh Quoc Ho, Benjamin Beker, Yi Chi Shih, and Yinchao Chen

***Abstract*—The spectral domain method is applied to study shielded microstrip resonators printed on anisotropic substrates. A Green's function that takes into account the dielectric anisotropy effects is derived through a fourth order formulation. Galerkin's method is then applied to form the characteristic equation from which the resonant frequency of the microstrip resonator is numerically obtained. Results**

Manuscript received March 12, 1991; revised November 8, 1991.

T. Q. Ho is with the Department of the Navy, NCCOSC, RDT&E Division, San Diego, CA 92152.

B. Beker, and Y. Chen are with the Department of Electrical and Computer Engineering, University of South Carolina, Columbia, SC 29208.

Y. C. Shih is with Hughes Aircraft Company, Industrial Electronics Group, M/S 235/1252, P.O. Box 2940, Torrance, CA 90509.

IEEE Log Number 9106038.

for a microstrip resonator situated on an isotropic substrate are used to validate the theory.

I. Introduction

Microstrip and disk resonators are among key important elements in the design of microwave and millimeter-wave frequency sources and filtering networks [1]. The analysis of such structures has been extensively investigated by numerous authors. Different methods based on various approximations [2] to the quasi-static approach [3]–[4] have been used to study these resonators. Since these analyses are based on approximations, which are inaccurate for high frequency applications, quite often a correction factor is needed in order to compensate for the dispersion effects. More accurate theories have been developed and implemented to study the characteristics of the microstrip resonators, as documented in [5]–[6]. Up until now, the emphasis of the resonator studies have been directed towards structures printed on isotropic materials, that is, the substrate being characterized by a zero-rank permittivity tensor.

In this paper, a full-wave analysis via the spectral domain approach is used to study the characteristics of shielded microstrip resonators printed on anisotropic substrates. The material is characterized by a second rank permittivity tensor in which all diagonal elements can be distinct. The Green's function of the structure is derived by applying the resonance conditions and by solving the fourth-order differential equations in the Fourier domain. A procedure based on Galerkin's method is then used to form the characteristic equation from which the resonant frequency of the resonator is numerically obtained. Data for a resonator printed on an isotropic substrate, which is treated as a special case of anisotropic, are computed and then compared to existing data, and good agreement is observed. The resonant frequencies of the microstrip resonators on anisotropic materials, such as PTFE cloth, boron nitride, epsilam-10, and sapphire are then computed.

II. Theory

The microstrip resonator structure under consideration is shown in Fig. 1 along with the coordinate system used. A rectangular strip of width w and length d is printed on one side of the anisotropic layer situated inside a shielded housing. For simplicity of the analysis, it is assumed that the operating frequency is below the cutoff frequency of the partially loaded waveguide. The substrate, which extends from $-b/2$ to $+b/2$, is also assumed to be lossless with thickness h_1. The distance from the microstrip resonator to the top cover is h_2. In general, the anisotropic medium is characterized by its permittivity tensor:

$$[\epsilon] = \epsilon_o \begin{vmatrix} \epsilon_{xx} & 0 & 0 \\ 0 & \epsilon_{yy} & 0 \\ 0 & 0 & \epsilon_{zz} \end{vmatrix} \quad \text{and} \quad [\mu] = \mu_o[1] \tag{1}$$

where ϵ_o and μ_o are the free-space values.

The vector wave equations for the components of the electric and magnetic fields within the anisotropic layer, which can be manipulated from Maxwell's equations, are expressed in their simplified forms as

$$\nabla X(\nabla X\boldsymbol{E}) - k_o^2[\epsilon] \cdot \boldsymbol{E} = 0 \tag{2a}$$

$$\nabla X([\epsilon]^{-1} \cdot \nabla X\boldsymbol{H}) - k_o^2\boldsymbol{H} = 0 \tag{2b}$$

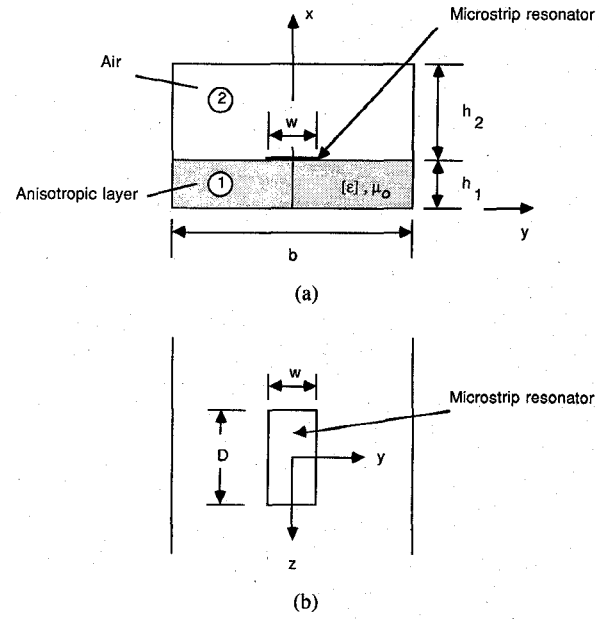

Fig. 1. Geometry of the shielded microstrip resonator. (a) End view. (b) Top view.

The Fourier transform of any quantity is defined through the following relation:

$$\tilde{\Psi}(x, \alpha, \beta) = \int_{-\infty}^{\infty} \int_{-b/2}^{b/2} \Psi(x, y, z) e^{j\alpha y} e^{j\beta z}\, dy\, dz \tag{3}$$

with α and β being the Fourier transform variables. When (2a) and (2b) are transformed according to (3) and reduced, a set of coupled differential equations written in terms of the tangential electric fields can be derived:

$$\frac{d^2\tilde{E}_y}{dx^2} + y_2\tilde{E}_y + y_4\tilde{E}_z = 0 \tag{4a}$$

$$\frac{d^2\tilde{E}_z}{dx^2} + z_2\tilde{E}_z + z_4\tilde{E}_y = 0 \tag{4b}$$

with y_2, y_4, z_2 and z_4 are the transformed coefficients. In order to find the solution for $\tilde{E}_y$ or $\tilde{E}_z$, (4a) and (4b) are then decoupled yielding a fourth order differential equation for either field. Once the tangential field solutions are found, the remaining components in the anisotropic region are then derived and they are expressed in their generalized forms as

$$\tilde{E}_z = A_n^* \sin(\gamma_+ x) + B_n^* \sin(\gamma_- x) \tag{5a}$$

$$\tilde{E}_y = E_y^+ A_n^* \sin(\gamma_+ x) + E_y^- B_n^* \sin(\gamma_- x) \tag{5b}$$

$$\tilde{H}_z = (j\omega\mu_o)^{-1} H_z^+ A_n^* \cos(\gamma_+ x) + (j\omega\mu_o)^{-1} H_z^- B_n^* \cos(\gamma_- x) \tag{5c}$$

$$\tilde{H}_y = (j\omega\mu_o)^{-1} H_y^+ A_n^* \cos(\gamma_+ x) + (j\omega\mu_o)^{-1} H_y^- B_n^* \cos(\gamma_- x) \tag{5d}$$

with

$$E_y^\pm = \{(\gamma_\pm)^2 - z_2\}/z_4 \tag{6a}$$

$$E_x^\pm = \frac{j}{\gamma_\pm}\left\{\alpha \frac{\epsilon_{yy}}{\epsilon_{xx}} E_y^\pm + \beta \frac{\epsilon_{zz}}{\epsilon_{xx}}\right\} \tag{6b}$$

$$H_y^{\pm} = \gamma_{\pm} - j\beta E_x^{\pm} \tag{6c}$$

$$H_z^{\pm} = -\gamma_{\pm} E_y^{\pm} + j\alpha E_x^{\pm} \tag{6d}$$

where $\gamma_{\pm}$ can be obtained by solving the fourth order characteristic equation through the method described in [7].

The fields within the isotropic region 2 can be derived based on the superposition of TE and TM fields. The transforms of the scalar potentials, which are used to find the field components, are written below:

$$\frac{d^2\tilde{\phi}^{e,h}}{dx^2} + (\gamma_2)^2\tilde{\phi}^{e,h} = 0. \tag{7}$$

After applying the boundary conditions at the top cover $x = h_1 + h_2$, the field expressions for region 2 are,

$$\tilde{E}_{y2} = \{c_1 A_n - c_2 B_n\} \sin \gamma_2(h_1 + h_2 - x) \tag{8a}$$

$$\tilde{E}_{z2} = c_3 B_n \sin \gamma_2(h_1 + h_2 - x) \tag{8b}$$

$$\tilde{H}_{y2} = \{c_4 A_n + c_5 B_n\} \cos \gamma_2(h_1 + h_2 - x) \tag{8c}$$

$$\tilde{H}_{z2} = c_6 A_n \cos \gamma_2(h_1 + h_2 - x) \tag{8d}$$

with c_1 to c_6 are the known constants.

At the air-anisotropic layer interface $x = h_1$, the appropriate boundary conditions are also imposed so that a set of matrix equations can be formed yielding the expression for the impedance Green's function:

$$\begin{vmatrix} \tilde{G}_{zz}(k_o, \alpha, \beta) & \tilde{G}_{zy}(k_o, \alpha, \beta) \\ \tilde{G}_{yz}(k_o, \alpha, \beta) & \tilde{G}_{yy}(k_o, \alpha, \beta) \end{vmatrix} \begin{vmatrix} \tilde{J}_z(\alpha, \beta) \\ \tilde{J}_y(\alpha, \beta) \end{vmatrix} = \begin{vmatrix} \tilde{E}_z(\alpha, \beta) \\ \tilde{E}_y(\alpha, \beta) \end{vmatrix} \tag{9a}$$

with the matrix elements defined as

$$\tilde{G}_{zz} = H_1/\det, \quad \tilde{G}_{zy} = -H_2/\det$$

$$\tilde{G}_{yz} = -H_3/\det, \quad \tilde{G}_{yy} = H_4/\det$$

$$\det = H_1 H_4 - H_2 H_3 \tag{9b}$$

where

$$H_1 = \xi_8 K^2 + \{-\xi_4 K^+ + \xi_3 K^-\}/\xi_{11} \tag{9c}$$

$$H_2 = \xi_7 K^2 + \{\xi_2 K^+ - \xi_1 K^-\}/\xi_{10} \tag{9d}$$

$$H_3 = \xi_7 K^2 + \{\xi_4\xi_5 K^+ - \xi_3\xi_6 K^-\}/\xi_{11} \tag{9e}$$

$$H_4 = \xi_9 K^2 + \{-\xi_2\xi_5 K^+ + \xi_1\xi_6 K^{-1}\}/\xi_{10} \tag{9f}$$

$$K^2 = \cot(\gamma_2 h_2), \tag{9g}$$

$$K^+ = \cot(\gamma_+ h_1), \tag{9h}$$

$$K^- = \cot(\gamma_- h_1). \tag{9i}$$

The remaining constants in (9c)–(9i), ξ_1 to ξ_{11}, can be written in terms of the transformed variables as well as the medium parameters.

To find the resonant frequency of the microstrip resonator, a procedure based on the Galerkin technique [6] is used, by first expanding the unknown currents $\tilde{J}_y$ and $\tilde{J}_z$ in terms of known basis functions:

$$\tilde{J}_y(\alpha, \beta) = \sum_{m=1}^{M} C_m \tilde{J}_{ym}(\alpha, \beta) \tag{10a}$$

$$\tilde{J}_z(\alpha, \beta) = \sum_{m=1}^{N} D_m \tilde{J}_{zm}(\alpha, \beta) \tag{10b}$$

and then, substituting $\tilde{J}_y$ and $\tilde{J}_z$ into the impedance Green's function (9a), and after taking the inner products with $\tilde{J}_{yi}$ and $\tilde{J}_{zi}$ for different indexes i, a set of algebraic equations is derived:

$$\sum_{m=1}^{M} T_{im}(1, 1) C_m + \sum_{m=1}^{N} T_{im}(1, 2) D_m = 0 \qquad i = 1, 2, 3, \cdots N$$

$$\sum_{m=1}^{M} T_{im}(2, 1) C_m + \sum_{m=1}^{N} T_{im}(2, 2) D_m = 0 \qquad i = 1, 2, 3, \cdots M \tag{11a}$$

with

$$T_{im}(1, 1)(k_o) = \sum_{n=1}^{\infty} \int_0^{\infty} \tilde{J}_{zi}(\alpha, \beta) \tilde{G}_{zz}(k_o, \alpha, \beta) \tilde{J}_{zm}(\alpha, \beta)\, d\beta \tag{11b}$$

$$T_{im}(1, 2)(k_o) = \sum_{n=1}^{\infty} \int_0^{\infty} \tilde{J}_{zi}(\alpha, \beta) \tilde{G}_{zy}(k_o, \alpha, \beta) \tilde{J}_{ym}(\alpha, \beta)\, d\beta \tag{11c}$$

$$T_{im}(2, 1)(k_o) = \sum_{n=1}^{\infty} \int_0^{\infty} \tilde{J}_{yi}(\alpha, \beta) \tilde{G}_{yz}(k_o, \alpha, \beta) \tilde{J}_{zm}(\alpha, \beta)\, d\beta \tag{11d}$$

$$T_{im}(2, 2)(k_o) = \sum_{n=1}^{\infty} \int_0^{\infty} \tilde{J}_{yi}(\alpha, \beta) \tilde{G}_{yy}(k_o, \alpha, \beta) \tilde{J}_{ym}(\alpha, \beta)\, d\beta. \tag{11e}$$

The right hand sides of (11a) have been eliminated in the Galerkin process through the application of Parseval's theorem. The simultaneous equations are then solved for the wave number k_o by setting the determinant of the coefficient matrix equal to zero and search for the root of the resulting equation.

For the dominant mode, $\tilde{J}_{y1}$ and $\tilde{J}_{z1}$ are chosen to have the following forms:

$$\tilde{J}_{y1}(\alpha, \beta) = \tilde{J}_1(\alpha)\tilde{J}_2(\beta) \tag{12a}$$

$$\tilde{J}_{z1}(\alpha, \beta) = \tilde{J}_3(\alpha)\tilde{J}_4(\beta) \tag{12b}$$

where the inverse transforms of $\tilde{J}_1$, $\tilde{J}_2$, $\tilde{J}_3$, and $\tilde{J}_4$ are given by

$$J_1 = \sin((2\pi y/w)/[1.0 - (2y/w)^2]^{1/2} \tag{12c}$$

$$J_2 = 2z/d^2 \tag{12d}$$

$$J_3 = 1.0 - (2y/w)^2]^{-1/2} \tag{12e}$$

$$J_4 = (2/d)\cos(\pi z/d). \tag{12f}$$

Note that the form of J_1 and J_3 is identical to the one used for computing the dispersive characteristics of infinitely long microstrip lines.

III. Results

To validate the theory, the resonant frequency of a shielded microstrip resonator printed on an isotropic substrate, which is treated as a special case of anisotropy, is computed and compared to published data. The dimensions of the structure are $b = 155.0$ mm, $h_1 = 12.7$ mm, $h_2 = 88.9$ mm, and $w = 20.0$ mm. The substrate is characterized by its permittivity tensor as $\epsilon_{xx} = \epsilon_{yy} = \epsilon_{zz} = 2.65$. Fig. 2 shows the response of the resonant frequency of the resonator with respect to different physical lengths. As can be seen, the resonator may resonate anywhere between 0.5 GHz to 0.8 GHz range, depending on the chosen dimensions. Plotted also with our data are the results reproduced from reference [6], and an excellent agreement is observed.

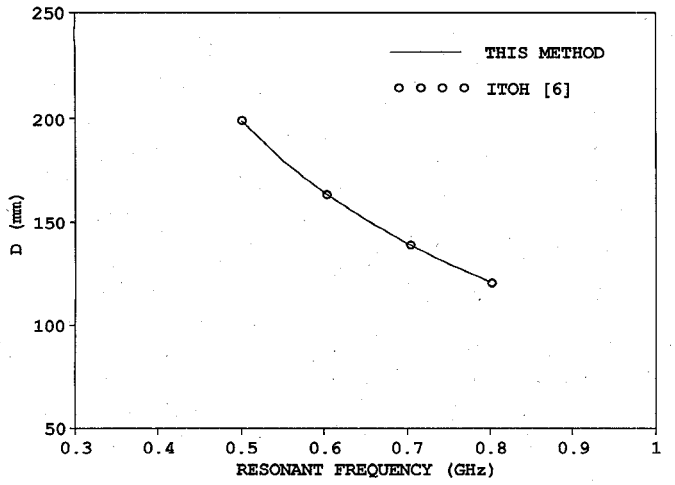

Fig. 2. Resonant frequency versus the resonator length with $\epsilon_{xx} = \epsilon_{yy} = \epsilon_{zz} = 2.65$, $b = 155.0$ mm, $h_1 = 12.7$ mm, $h_2 = 88.9$ mm, and $w = 20.0$ mm.

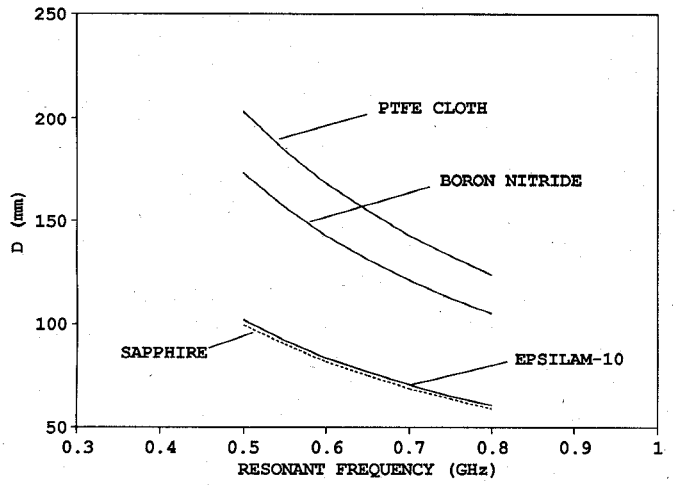

Fig. 3. Resonant frequency of the microstrip resonator printed on anisotropic substrates with $b = 155.0$ mm, $h_1 = 12.7$ mm, $h_2 = 88.9$ mm, and $w = 20.0$ mm.

Next, the data for microstrip resonators printed on anisotropic substrates are computed. For the biaxial substrate, namely PTFE cloth, the medium parameters are $\epsilon_{xx} = 2.45$, $\epsilon_{yy} = 2.89$, and $\epsilon_{zz} = 2.95$. For the uniaxial cases, they are specified as $\epsilon_{xx} = 3.4$ and $\epsilon_{yy} = \epsilon_{zz} = 5.12$, $\epsilon_{xx} = 10.3$ and $\epsilon_{yy} = \epsilon_{zz} = 13.0$, and $\epsilon_{xx} = 11.6$ and $\epsilon_{yy} = \epsilon_{zz} = 9.4$, written respectively for boron nitride, epsilam-10, and sapphire. Fig. 3 shows how the resonant frequency responds when various materials are used. Note that the physical parameters used here are the same as for those previously specified for the resonator printed on the isotropic substrate. The results show that by changing the medium from PTFE cloth to boron nitride, the resonant frequency reduces considerably, and this is in contrast to what happens when the medium changes from epsilam-10 to sapphire. In the second case, only a small variation in resonant frequency is observed. This behavior can be confirmed by using transmission line theory, where the resonant frequencies of the resonators are approximated by $(\lambda_o/2)/\sqrt{\epsilon_{\text{eff}}}$. Since the effective dielectric constant of an infinitely long microstrip line on epsilam-10 is very close to that computed for the sapphire substrate, this implies that the resonant frequencies of the resonators for these two media are just about the same.

IV. Conclusion

An analysis based on the spectral domain method applied to study shielded microstrip resonators printed on anisotropic materials was presented. The anisotropic layer is generally specified by its second rank permittivity tensor. The Green's function for the structure is obtained through a fourth order D. E. formulation. Galerkin's method testing procedure in the Fourier domain is applied to form the characteristic equation from which the resonant frequency of the resonator is numerically obtained. Data on the resonant frequency of resonators printed on both uniaxial and biaxial substrates were also generated.

References

[1] M. V. Schneider, "Millimeter-wave integrated circuits," *IEEE G-MTT Int. Symp. Microwaves*, June 1973.
[2] S. Mao, S. Jones, and G. D. Vendelin, "Millimeter-wave integrated circuits," *IEEE Trans. Microwave Theory Tech.*, vol. MTT-16, pp. 455–461, July 1968.
[3] J. Wolff and N. Knoppik, "Rectangular and circular microstrip disc capacitors and resonators," in *Proc. European Microwave Conf.*, Brussels, Belgium, Sept. 1973.
[4] T. Itoh and R. Mittra, "Analysis of a microstrip disk resonator," *Arch. Eleck. Ubertagung.*, vol. 27, pp. 456–458, Nov. 1973.
[5] ——, "A technique for computing dispersion characteristics of shielded microstrip lines," *IEEE Trans. Microwave Theory Tech.*, vol. MTT-22, pp. 896–898, Oct. 1974.
[6] T. Itoh, "Analysis of microstrip resonator," *IEEE Trans. Microwave Theory Tech.*, vol. MTT-22, pp. 946–952, Nov. 1974.
[7] T. Q. Ho and B. Beker, "Spectral domain analysis of shielded microstrip lines on biaxially anisotropic substrates," *IEEE Trans. Microwave Theory Tech.*, vol. 39, pp. 1017–1021, June 1991.

Analysis of a Coupled Slotline on a Double-Layered Substrate Containing a Magnetized Ferrite

Masahiro Geshiro and Tatsuo Itoh

***Abstract*—Nonreciprocity in the propagation characteristics of the even and odd modes in magnetized-ferrite-loaded double-layered coupled slotlines is studied. The analysis is based on Galerkin's method applied in the Fourier transform domain. Numerical results are presented for various values of structural parameters. As a result, it is found that the waveguide structures studied have sufficient nonreciprocity in propagation constants for isolators and four port circulators.**

I. Introduction

Slotlines are well suited for their usage in nonreciprocal ferrite devices for microwave integrated circuits since the magnetic field has elliptical polarization [1]. Recently, several analytical methods for propagation characteristics in slotlines and finlines containing

Manuscript received May 14, 1991; revised October 30, 1991.

M. Geshiro is with the Department of Electronics, Ehime University, Bunkyo-3, Matsuyama, Ehime 790, Japan.
T. Itoh is with the Department of Electrical Engineering, The University of California at Los Angeles, 66-147A Engineering IV, Los Angeles, CA 90024-1594.

IEEE Log Number 9106046.